

**REVIEW****Use and Effect of Si/Silica Nano Materials in Polyurethane's Structure**

A. SHOKUHI RAD\* and M. ARDJMAND

*Department of Chemical Engineering, South Tehran Branch**Graduate Faculty, Islamic Azad University, Tehran, Iran**Tel/Fax: (98)(216)6259470; E-mail: shokohiradali@yahoo.com*

Polyurethanes are functional polymers whose properties can be tailored made by simply adjusting the compositions to meet the highly diversified demands of modern technology. The assembly of inorganic-organic nanocomposite materials affords unique opportunities to create revolutionary material combinations. These novel materials can have unexpected properties arising from the synergism between the components. More and more attention is being paid to the incorporation of an inorganic network such as a silica phase into an organic polymer matrix because of the potential physical and chemical properties. In the past decade, material scientists showed great interest in organic-inorganic nanocomposites as their application could dramatically improve material properties such as heat resistance, radiation resistance, mechanical and electrical properties and other properties in engineering plastics, enhanced rubber, coatings and adhesives. The properties of nano-composites strongly depend on the organic matrix, nanoparticles and the way in which they were prepared. Many researchers studied organic/inorganic nanocomposite systems and tried to understand the mechanism so as to obtain the expected improvement over traditional organic materials. It was founded that nano-silica could increase the hardness and scratch resistance of a coating and keep it clear at the same time. Nano-silica could enhance tensile strength and elongation of polyurethanes elastomer, although the modulus and hardness were lower than the corresponding microsize filled polyurethanes.

**Key Words:** SiO<sub>2</sub>, Clay, Silicate, Polyurethane, Nanocomposite.

**INTRODUCTION**

Polyurethane is a segmented block copolymer composed of alternating hard and soft segments. Polyurethane has been extensively used due to its excellent physical properties, *e.g.* flexibility at low temperature, abrasion resistance, variable hardness, *etc.* However, polyurethane has drawbacks of low thermal stability and mechanical strength. A great deal of effort has been devoted to improving its properties in recent years, which includes chemical modification to its molecular structure and addition of inorganic filler (including clay and wollastonite). In general, the addition of inorganic filler can strengthen polymer matrix without improving its toughness or even reducing its elongation at break<sup>1-4</sup>.

More and more attention is being paid to the incorporation of an inorganic network such as a silica phase into an organic polymer matrix because of the potential physical and chemical properties<sup>5-10</sup>. There are many methods for attaching polymer chains onto nanoparticle surfaces, including chemisorption<sup>11</sup>, the covalent attachment of end-functionalized polymers to a reactive surface (grafting-to)<sup>12</sup> and *in situ* monomer polymerization with the monomer growth of polymer chains from immobilized initiators (grafting from)<sup>13,14</sup>.

Solvent and waterbased polyurethanes are modified to make it as advanced materials either by varying polyurethane microstructures or by dispersing inorganic fillers, especially through incorporation of nano-sized layered silicates within the polyurethane continuous matrix. MMT, a layered silicate with lamellar shape, has attracted intensive research interest recently, for the preparation of polyurethane/clay nanocomposites. This is because the lamellar platelets of MMT display high in-plane strength, stiffness and aspect ratio<sup>15,16</sup>. Depending upon the organization of the silicate layers in a polymer matrix, two types of morphology can be achieved in the nanocomposites *i.e.*, intercalated or exfoliated. In general, there are various methods that can be used to prepare polymer/montmorillonite; exfoliation-adsorption, *in situ* intercalative polymerization, melts intercalation and template synthesis<sup>17-23</sup>. After the development of the nylon/MMT nanocomposite<sup>24</sup>, a large number of new polymer/clay nanocomposites based have been investigated<sup>25-30</sup>.

Inorganic-organic nanocomposites can be prepared by directly blending organic materials with inorganic nanoparticles or by a sol-gel process with a metal alkoxide such as tetraethoxysilane (TEOS) for the silicon dioxide (SiO<sub>2</sub>)-polymer system. The most commonly used inorganic nanoparticles are SiO<sub>2</sub>, TiO<sub>2</sub>, ZnO and CaCO<sub>3</sub>. Of these, nano-silica was first produced and studied in a number of polymer systems. For instance, Chang *et al.*<sup>23,31</sup> introduced it into a poly(methyl methacrylate) matrix.

There are many papers in the literature about solvent-based polyurethane/clay nanocomposites. These research papers have described the effect of incorporation of nanolayers of mineral clay on the thermal stability<sup>32-34</sup>, mechanical strength<sup>35-37</sup>, morphology and elasticity<sup>23</sup> properties of these nanocomposites. Long chain organoammonium compounds are widely used in the modification of pristine clay and there are relatively few reports on the modification of clay by organosilanes<sup>38,39</sup>.

It has been well established that the introduction of SiO<sub>2</sub> into a polymer matrix can effectively improve the polymer's properties such as abrasion resistance, shock absorption, surface hardness, modulus and so on. However, it is difficult for nano-silica particles to be dispersed directly in the water phase without a surface pre-treatment such as graft modification by a organosilane coupler<sup>40,41</sup>. Even though they can be dispersed temporarily, the nano-silica particles gather together in larger aggregates finally because of their high surface energy.

To achieve the expected improvement by adding nanocomposites, understanding how these nanoparticles influence the organic matrix is important. Organic-inorganic nanocomposites can be prepared by directly blending with nanoparticles and organic

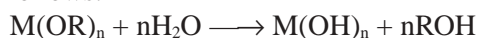
compounds or a sol-gel process with a metal alkoxide. The most commonly used inorganic nanoparticles are SiO<sub>2</sub>, TiO<sub>2</sub>, ZnO, CaCO<sub>3</sub>, *etc.*, of them, nano-silica is the first nanoparticle produced and has been studied in a lot of polymer systems. For example, Kaddami *et al.*<sup>42</sup> and Hajji *et al.*<sup>43</sup> had combined it with poly(HEMA) and Chang *et al.*<sup>44</sup> filled it into poly(methyl methacrylate). Nano-silica could also improve scratch resistance of a coating and keep the coating clear at the same time<sup>45</sup>. Petrovic *et al.*<sup>46</sup> found that nanoparticle could enhance tensile strength and elongation of polyurethane elastomer. In this project, nano-silica was embedded in the acrylic-based polyurethane, composition of the coatings at the surface and at the interface, hardness, abrasion resistance, static and dynamic mechanical properties, scratch resistance and optical properties of the coatings were intensively investigated by X-ray photoelectron spectrometer (XPS), pendulum hardness tester, Nano-Indenter XP, Instron testing machine, dynamic mechanical analyzer (DMA), transmission electron micrograph (TEM) and UV-Vis spectrophotometer. For the sake of comparison, the effects of fumed silica and micro-silica on polyurethane properties were also studied.

#### Preparation of silicon dioxide/polyurethane

**By sol-gel process:** The SiO<sub>2</sub>/polyurethane nanocomposites in which cationic polyurethane was presented in a form of a microemulsion were developed to reduce the surface energy of nano-silica<sup>23</sup>.

Organic-inorganic nanocomposites combine the advantages of organic polymers (flexibility, ductility, dielectric strength, *etc.*) and those of inorganic materials (rigidity, high thermal stability, UV-shielding property and high refractive index, *etc.*)<sup>47-55</sup>. Moreover, they usually contain some special properties of nanoparticles and consequently can be widely used in many fields such as plastics, rubbers, coatings, inks and so forth. Generally, there are two typical kinds of organic-inorganic nanocomposites, depending on the strength or level of interaction between organic and inorganic phases: one involving physical or weak phase interaction (*e.g.*, hydrogen bonding, van der Waals forces) and another possessing a strong chemical covalent or ionic-covalent bond between the organic and inorganic phases. The typical preparation method, for the second kind of organic-inorganic nanocomposites, is the so-called sol-gel technique. There are many nanocomposite polymers, especially containing nano-SiO<sub>2</sub> or nano-TiO<sub>2</sub>, prepared by sol-gel approach and investigated by focusing on how the nanoparticles influence mechanical, thermal and optical properties and so on, of the nanocomposite polymers and the relationship between structure and properties.

Since the 1970s the sol-gel process has been used for the deposition of inorganic minerals *in situ* in an organic polymer matrix<sup>56,57</sup>. Starting materials for the sol-gel process are metal alkoxides, M(OR)<sub>n</sub> and a small amount of acid or base as catalyst. Metal alkoxides are hydrolyzed and metal hydroxides, M(OH)<sub>n</sub>, are formed. The reaction is shown as follows:



where  $M = \text{Na, Ba, Cu, Al, Si, Ti, Ge, V, W}$ ,  $R = \text{CH}_3, \text{C}_2\text{H}_5, \text{C}_3\text{H}_7, \text{C}_4\text{H}_9, \dots$ ;  $\text{M}(\text{OH})_n$  are reactive and threedimensional networks with  $-\text{OOMOOOM}-$  linkages, formed by polycondensation<sup>58</sup> of  $\text{M}(\text{OH})_n$  with  $\text{M}(\text{OR})_n$  or  $\text{M}(\text{OH})_n$ .

The diagrammatic sketch of micelles formed by cationic polyurethane ionomers in water is shown in Fig. 1. According to the conclusion suggested by Lorenz<sup>59-61</sup> cationic polyurethane ionomers in water are stabilized because of the electric double layer and solvent effect. Because the soft segment of cationic polyurethane is hydrophobic and the hard segment with  $\text{NH}_2^+$  is hydrophilic, the molecular chains of cationic polyurethane can self-organize to micelles when dispersed in water. The hydrophilic groups in the micelles are on the surfaces of particles and hydrophobic groups are crimped into the particles. The micelles make a Brownian motion and positive charges are simultaneous with negative ones, so an electric double layer is formed on the surface and there is a voltage between them. The voltage blocks the aggregation of particles, causing them to act as a surfactant. At the same time, there are hydrogen bonds between the hydrophilic groups and water molecules and then the particles are surrounded by a layer of water molecules.

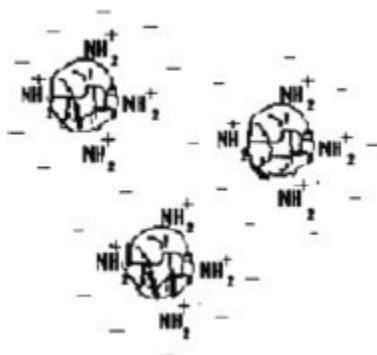


Fig. 1. Diagrammatic sketch of micelles formed by cationic polyurethane ionomers in water [Ref. 23]

The microdomain structures of the polyurethane and  $\text{SiO}_2$ /polyurethane were analyzed by FTIR as shown in Fig. 2. From Fig. 2, the peaks that are characteristic of polyurethane structure may be found in the curves for both polyurethane and  $\text{SiO}_2$ /polyurethane systems. In addition, there were some other peaks in the IR spectra of  $\text{SiO}_2$ /polyurethane. The peak with a wave number of  $3384 \text{ cm}^{-1}$ ; corresponded to O-H stretching of Si-OH and the peaks at  $1100$  and  $871 \text{ cm}^{-1}$  were attributed to SiOO stretching. It may thus be proved that the structure of polyurethane was been affected by the presence of  $\text{SiO}_2$ , implying that the  $\text{SiO}_2$  did not react with the polyurethane molecules. From which it may be seen that the silicon element was in the sample in addition to carbon and oxygen. As we know, there were no charges on the surface of  $\text{SiO}_2$ ; thus  $\text{SiO}_2$  particles themselves could not move toward the negative electrode automatically during the electrophoresis process except by being encapsulated

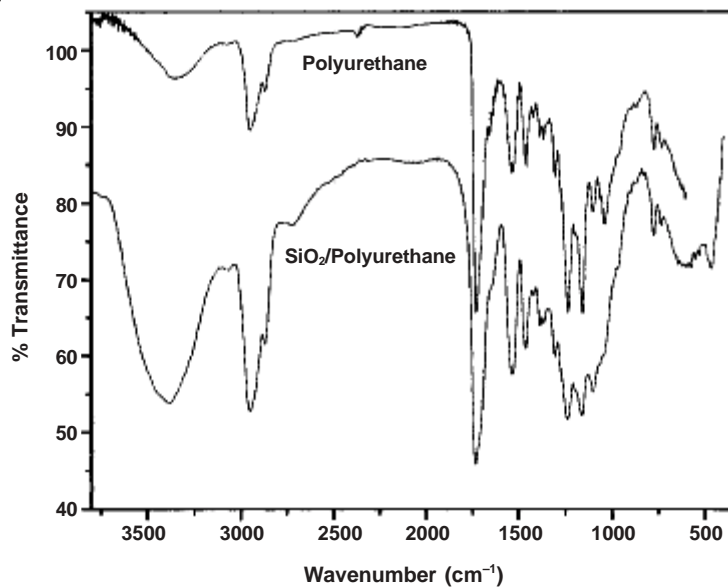


Fig. 2. FTIR spectra of pure polyurethane and SiO<sub>2</sub>/polyurethane nanocomposite with the ratio of 3:10 by weight between tetraethoxy silane and polyurethane [Ref. 23]

by cationic polyurethane micelles. Thus, we can say that TEOS had precipitated *in situ* in the polyurethane matrix and then SiO<sub>2</sub>/polyurethane nanocomposites could be prepared by this method. Fig. 3 is the TEM micrograph of SiO<sub>2</sub>/polyurethane nanocomposite coloured by phosphor wolframic acid. We can see clearly that the SiO<sub>2</sub>/polyurethane nanocomposite particle is approximately round with a diameter of about 90-100 nm.



Fig. 3. TEM image of SiO<sub>2</sub>/polyurethane nanocomposite with the ratio of 2:10 by weight between tetraethoxy silane and polyurethane

The particle size of SiO<sub>2</sub>/polyurethane was reported larger than that of polyurethane and the distribution wider. The size actually doubled going from pure polyurethane to SiO<sub>2</sub>/polyurethane nanoparticles. This is because polyurethane micelles could effectively encapsulate TEOS, supplying microreactors for its hydrolysis and polycondensation. The electric double layer and solvent effect would block the aggregation of particles. However, because the nanoparticles were of a loose structure in which there were other materials such as water and alcohol besides SiO<sub>2</sub> particles, the precipitation of TEOS within polyurethane nanocapsules caused the particles to increase in diameter. Even so, both of them were still at the order of nanometer.

**Frontal polymerization:** Frontal polymerization (FP) is a mode of converting a monomer into a polymer *via* a localized reaction zone that propagates through the monomer<sup>62</sup>. The first frontal polymerization reactions were discovered in Russia by Chechilo and Enikolopyan in 1972, who studied methyl methacrylate polymerization under high pressure<sup>63-65</sup>. The method was later extended by Pojman and coworkers to include numerous polymers<sup>66-70</sup>. Pojman and coworkers have done a great deal of work focusing on the feasibility of traveling fronts in solutions of thermal free-radical initiators in a variety of neat monomers at ambient pressure with liquid monomers<sup>71,72</sup> or a solid monomer<sup>21</sup>. The majority of frontal polymerization work has been performed on a free-radical polymerization system because it is usually highly exothermic and the heat of the reaction provides autocatalysis for a polymerization front propagating through a liquid monomer. However, it is not the only system. The frontal curing of epoxy resins has been investigated<sup>73,74</sup>. Begishev *et al.*<sup>75</sup> studied the frontal anionic polymerization of caprolactam. Frontal ring-opening metathesis polymerization has been successfully achieved with dicyclopentadiene and has been applied to making interpenetrating networks<sup>76,77</sup>. Recently, much of the research in this field has been devoted to the study of frontal polymerization<sup>78-80</sup>. Mariani and coworkers<sup>23,30</sup> prepared polyurethanes frontally with 1,6-hexamethylene diisocyanate and ethylene glycol and prepared interpenetrating polydicyclopentadiene-polyacrylate networks *via* frontal polymerization. Fiori *et al.*<sup>81</sup> synthesized polyacrylate/poly(dicyclopentadiene) networks frontally. Frontal atom transfer radical polymerization has also been achieved<sup>82</sup>. Because of the large thermal and concentration gradients, polymerization fronts are highly susceptible to buoyancy-induced convection. Descending fronts of thermoset formation are normally immune to convection unless the reactor is tilted with respect to the gravitational vector<sup>83</sup>. Pojman *et al.* demonstrated possible methods for overcoming the instabilities by adding fillers<sup>84</sup> and performing the fronts in weightlessness<sup>85</sup> polyurethanes provide a wide range of properties from a variety of starting materials. Tailor-made properties of these materials can be obtained from combinations of monomeric materials. On a molecular basis, a polyurethane may be described as a linear-structure block copolymer of the (AB)<sub>n</sub> type. Part A, the hard segment, is composed of oligomers, which are prepared through the reaction of a low-molecular-weight diol or triol chain extender with a diisocyanate. Part B, the soft segment, is normally a polyester or a polyether polyol with a molecular weight of 1000-3000<sup>86</sup>.

Some research groups have prepared polyurethane composites containing intercalated silicate layers<sup>86-90</sup> and silica<sup>91-101</sup>. Goda and Frank<sup>35</sup> studied the effect of the organoclay concentration on the properties of polyurethane-clay nanocomposites. Martin-Martinez *et al.*<sup>91</sup> studied polyurethanes containing different types of silicas. They used silicas as fillers in thermoplastic polyurethane composites. The physical properties of the polyurethane-silica composites and the interactions between the silica and polyurethane were investigated. In this article, we report on the preparation of polyurethane and polyurethane-silica hybrid nanocomposites with poly(propylene oxide) glycol (PPG) and the chain extender 1,4-butanediol (BD) by frontal polymerization. Nano-silica was used to increase the viscosity of the solution to result in a more stable front and with the idea of preparing useful materials. Materials were also prepared by batch polymerization (BP) with stirring.

**Morphology:** A TEM micrograph of polyurethane film with 3 wt % nano silica is shown in Fig. 4 and indicates that most of the nano-silica particles are evenly dispersed at the scale of  $\approx 100$  nm in the composite film, but that some aggregates can still be observed, although *in situ* polymerization was employed<sup>102</sup>. This is because nano-silica particles have much stronger hydrogen bonding through -OH groups and higher surface free energy in comparison with micro silica and thus tend to aggregate. Topographic images of the nanocomposite polyurethane/iron interface were observed by AFM. Fig. 5a,b show the topographic images of the interface of pure polyurethane cured at room temperature ( $^{\circ}\text{C}$ ), respectively. The polyurethane film cured at room temperature has a rough morphology at its interface, whereas the polyurethane film cured at  $100^{\circ}\text{C}$  has some holes, 250-500 nm in diameter, at the interface<sup>107</sup>. When the polyurethane was embedded with a small amount of nano-silica, *e.g.*, 1 wt %, the polyurethane interface displayed some hemispherical aggregates whose size was around 100 nm, as shown in Fig. 5c. As the nano-silica content was increased to 7 wt %, these hemispherical aggregates with the size of  $\approx 100$  nm could still be observed at the polyurethane interface, as illustrated in Fig. 5d. These hemispherical aggregates should be nano-silica particles, based on FTIR-ATR analysis and TEM observation. The Ra and RMS values of different polyurethane interfaces are summarized in Table-1. The data show that

TABLE-1  
PHYSICAL AND MECHANICAL PROPERTIES OF POLYESTER RESIN AND  
POLYURETHANE WITH VARIABLE NANO-SILICA CONTENT [Ref. 104]

Content (wt %)	Viscosity (mPa s)	Macro hardness
0	1100	0.11
1	1510	0.28
3	3800	0.38
3*	3100	–
5	6420	0.42
7	8340	0.52

\*By blending.

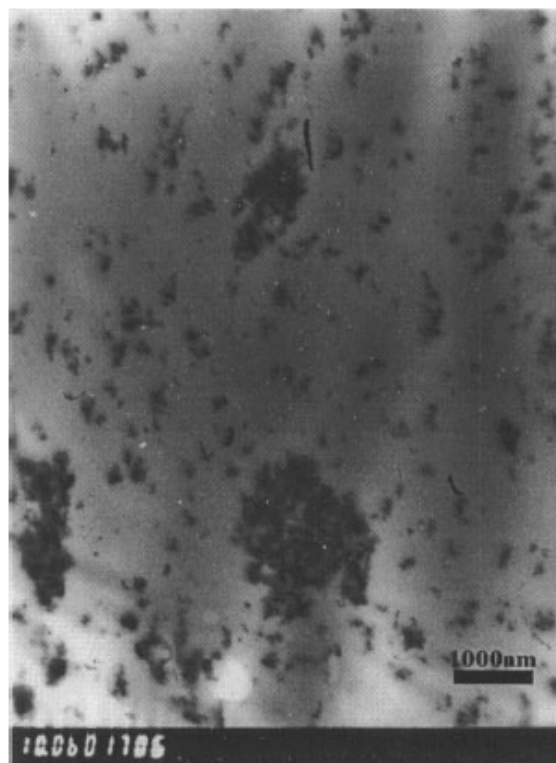


Fig. 4. TEM micrograph of nanocomposite polyurethane with 3 wt % nano-silica [Ref. 104]

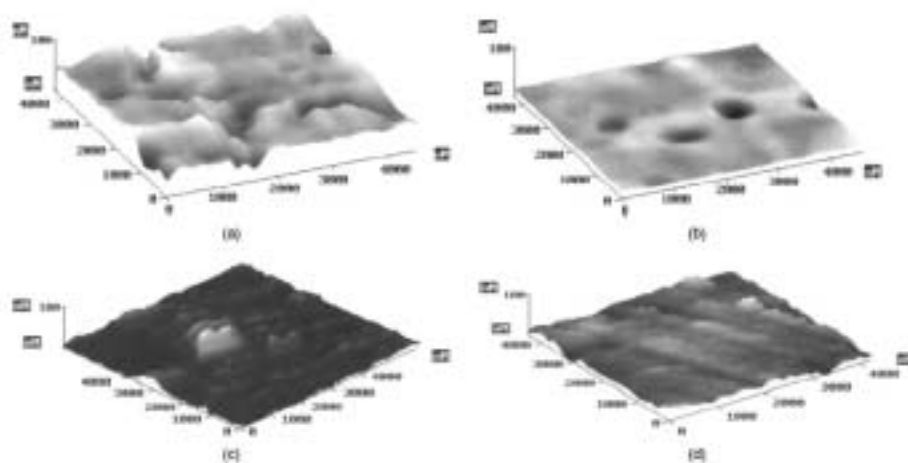


Fig. 5. AFM topographic images of polyurethane/substrate interfaces: (a) with 0 wt % nano-silica cured at room temperature; (b) with 0 wt% nano-silica cured at 100 °C; (c) with 1 wt % nano-silica cured at room temperature; (d) with 7 wt % nano-silica cured at room temperature [Ref. 102]



the Ra and RMS of the interface of nanocomposite polyurethane, even if containing only 1 wt % nano-silica and cured at room temperature, are considerably greater than those of pure polyurethane interfaces. As discussed previously, the interface roughness could be considered as the index of interface adhesion strength<sup>103</sup>. The adhesion strength of polyurethane interface containing nano-silica is considerably higher than that of polyurethane interface without nano-silica, as reported by Xichong and Wu<sup>102</sup>. It gives a hint that introducing nano-silica particles could possibly be more effective in improving adhesion strength than increasing the curing temperature. The nano-silica content seems to have no obvious impact on Ra, RMS and adhesion strength of polyurethane interfaces, suggesting that 1 wt % nano-silica could possibly occupy all the polyurethane interface top layer.

### Physical and mechanical properties

**Glass-transition temperatures of polyurethane/nano-silica composites:** Loss  $\tan \delta$  curves of polyurethane films, as a function of temperature, can be obtained by DMA measurement<sup>104</sup>.

Fig. 6 shows the DMA curve of pure polyurethane. The  $\tan \delta$  peak, at around 42 °C reflects the micro-Brownian segmental motion of amorphous polyester segment is defined as the glass-transition temperature ( $T_g$ ). Fig. 7 illustrates the effects of silica particle size and preparation method on the  $T_g$  values of nanocomposite polyurethane films. As the silica particles are introduced, the  $T_g$  values of polyurethane/nano-silica composites clearly increase compared with pure polyurethane, no matter which silica particles or preparation approaches are used. The  $T_g$  values of polyurethane/nano-silica composites first increase then decrease as the particle size increases. The maximum  $T_g$  values occur at silica particle sizes within the range of 28-66 nm, which is very consistent with the variation of hydroxyl values at the surfaces of silica particles, as shown in Table-1. Because the nano-silica with sizes of

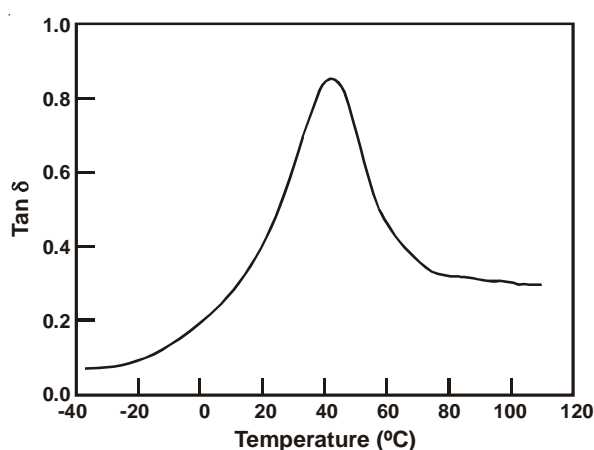


Fig. 6. Loss  $\tan \delta$  curve of pure polyurethane film as a function of temperature [Ref .104]

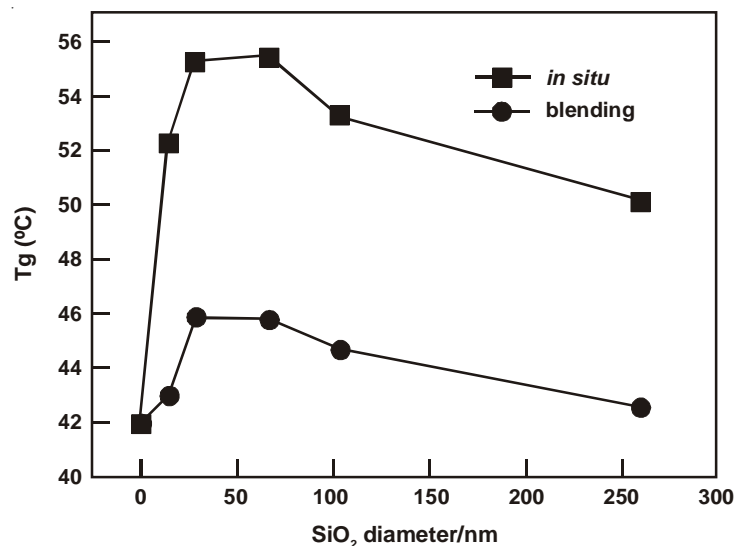


Fig. 7. Effect of silica particle size on the  $T_g$  of polyurethane/nano-silica composites with 2.25 wt %  $\text{SiO}_2$  content [Ref. 104]

28-66 nm have the highest  $-\text{OH}$  values at their surfaces among these particles, they should have the strongest interaction with macromolecular chains by hydrogen bonding or chemical action between  $-\text{OH}$  groups of silanol and  $-\text{OH}$  or  $-\text{COOH}$  groups from resin molecules at the same mass level, restricting the segmental motion of amorphous polyester molecular chains. Fig. 4 also reveals that the polyurethane/nano-silica composites, obtained from *in situ* polymerization, have much higher  $T_g$  values than those of their corresponding composites from the blending method because more polyester segments were chemically bonded to silica particles during *in situ* polymerization than during the blending method, as discussed above.

The effect of nano-silica on the viscosity of polyester resin and the mechanical properties of polyurethane films were investigated and are presented in Table-1. As the nano-silica content increases, the viscosity of polyester resin increases. To investigate how the nano-silica content influences the viscosity of the polyester resin, the same polyester resin was blended with 3 wt % nano-silica and its viscosity was around 3100 mPa s, also listed in Table-1, 700 m Pas lower than that of polyester resin with 3 wt % nano-silica obtained through *in situ* polymerization. This suggests that the increase in viscosity is not only caused by the physical interaction but stems also from the chemical bonding action between polyester resin molecules and nano-silica particles. The data in Table-1 also shows that increasing the nano-silica content can increase the hardness of polyurethane film. The change in mechanical loss tangent,  $\tan \delta$ , was compared by Chen<sup>62</sup> as a function of temperature before and after nano-silica particles were embedded in polyurethane film. The  $\alpha$  absorption was observed at 10 °C and 25 °C for polyurethane without and with 3 wt % nano-silica

embedded, respectively. The  $\alpha$ -absorption arises from micro-Brownian segmental motion of amorphous polyester molecular chains associated with the glass transition<sup>12</sup>. As more nano-silica is used, the  $\alpha$ -absorption temperature increases, namely, the  $T_g$  of the soft segments increases, indicating that nano-silica particles could effectively act as reinforced fillers because of their much larger surface area and stronger interaction with resin molecules, as compared with micro-silica particles.

**Effect of the nan-silica content on the polyester's viscosity:** The viscosities of the polyester resins *versus* their nano-silica contents are shown in Fig. 8. In comparison with the pure polyester resin, the polyester resin containing nano-silica had an increased viscosity. Moreover, the rate of increase, that is, the slope of the curve, increased with the nano-silica content. This was attributable to the fact that more hydrogen bonds between the O-H groups in the polyester resins and nano-silica particles were formed as the nano-silica content was increased.

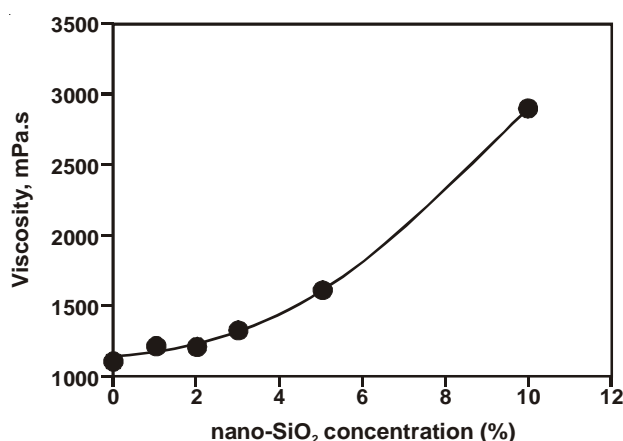


Fig. 8. Dependence of the viscosity of the polyester resins on the nano-silica content [Ref. 105]

**Effects of nano-SiO<sub>2</sub> particles on the macrohardness of polyurethane:** Table-2 summarizes the effects of nano-SiO<sub>2</sub> particles on the macro-hardness of polyurethane films. The data shows that the hardness first increased and then decreased as the nano-SiO<sub>2</sub> content increased further, no matter how much the film thickness changed. The MIH of the polyester-based films was measured with a modified scanning probe microscope equipped with a conical diamond tip. The introduction of a small amount of nano-SiO<sub>2</sub> into the polyester resin led to an increase in the MIH, no matter which polyester composition and which type of curing agent were used. The case of resin A cured with IPDI indicated that the MIH increased as the nano-silica content increased and this was partially consistent with the variation of the macrohardness. The weight losses of the polyurethane films before and after nano-silica was added are shown in Fig. 9, which indicates that polyurethane containing

TABLE-2  
EFFECT OF NANO-SiO<sub>2</sub> CONTENT ON THE MACROHARDNESS  
OF POLYURETHANE COATINGS [Ref. 105]

Nano-SiO <sub>2</sub> content (%)	Macro-hardness* (#60 drawdown rod)	Macro-hardness** (#100 drawdown rod)
0	0.48	0.41
1	0.62	0.44
3	0.63	0.34
5	0.59	0.29
10	0.50	0.37

\*The thickness of the films was about 30 μm and the films were dried for 1 day.

\*\*The thickness of the films was about 50 μm and the films were dried for 4 days.

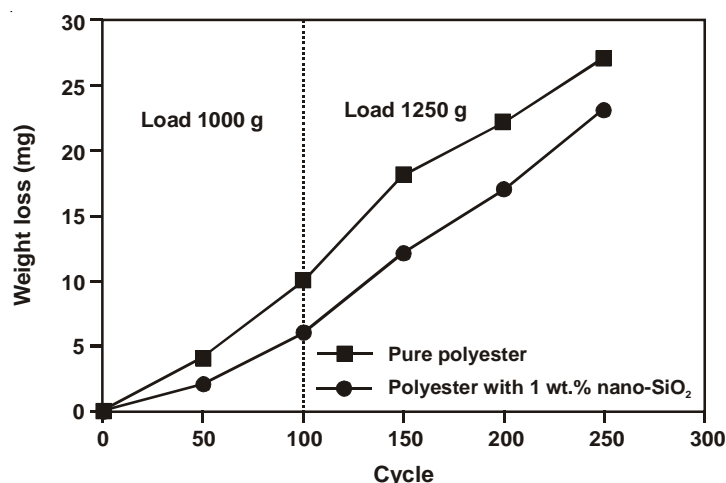


Fig. 9. Effect of the nano-silica on the weight loss of the polyester-based polyurethane films [Ref. 105]

1 wt % nano-SiO<sub>2</sub> had better abrasion resistance than pure polyurethane. However, the abrasion resistance decreased with an increasing content of nano-SiO<sub>2</sub> until the content reached 10 wt %, as reported by Zhou *et al.*<sup>105</sup>.

**Abrasion resistance:** The weight loss of the polyurethane films with different nano-silica content at different abrasion cycle is shown in Fig. 10. The weight loss gradually decreases as nano-silica content increases, indicating that nano-silica can improve the abrasion resistance of the coating film. Figs. 11 and 12 manifest the effect of the types of silica and micro-silica content on the weight loss of film, respectively. It was seen from Fig. 11 that the abrasion resistance of the films containing different types of silica are nearly the same except for the fumed silica. Fig. 12 shows that the weight loss does not change if only a small amount of micro-silica (*e.g.* 1 wt. %) is added, but the abrasion resistance increases as micro-silica content increases.

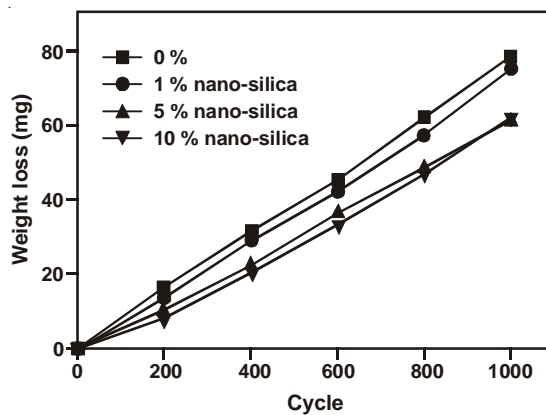


Fig. 10 Weight loss of the polyurethane films containing different nano-silica content [Ref. 106]

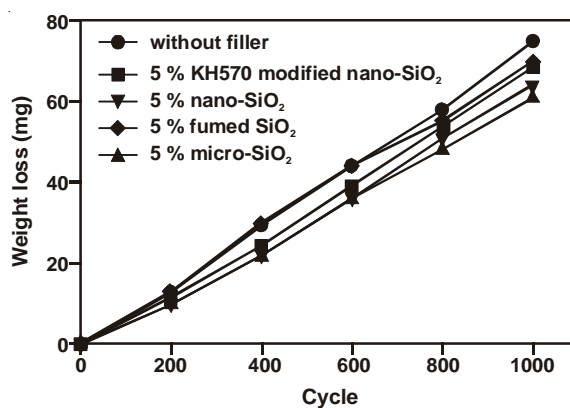


Fig. 11. Weight loss of the polyurethane films containing different types of silica [Ref. 106]

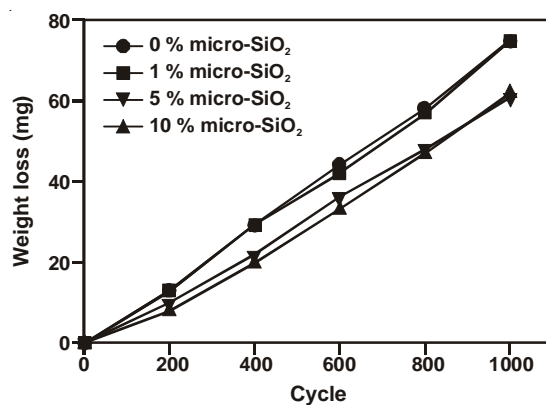


Fig. 12. Weight loss of the polyurethane films containing different micro-silica content [Ref. 106]

**Silicon element in composition of the surface and interface:** The composition of the surface and interface of polyurethane films containing 5 wt. % nano-silica or microsilica were determined by XPS by shuxue<sup>106</sup>. The results are listed in Table-3. There is no silicon element detected at the surfaces and interfaces of the films, no matter nano-silica or micro-silica particles are contained in the films, suggesting that silica are not like organic silanizing compounds in which silicon segments prefer to orient at the surface, silica like to immigrate into the bulk. The interfaces contain N element while the surfaces have no N element, indicating that urethane segments intend to orientate at interfaces while acrylic segments like to cover the surface since the former have higher free surface energy than the latter<sup>106</sup>. The N content at the interface of the film containing nano-silica is lower than that of micro-silica. This is possibly because nano-silica have considerably greater specific area than micro-silica and the -OH groups on the surfaces of nano-silica can react with -NCO groups from HDI, resulting in more -NCO groups absorbed on the surfaces of nano-silica, which like to hide into the bulk.

TABLE-3  
COMPOSITION OF THE SURFACE AND INTERFACE OF POLYURETHANE  
COATS CONTAINING NANO- OR MICRO-SILICA (at. %)

Element	Surface		Interface	
	Nano-silica	Micro-silica	Nano-silica	Micro-silica
C	69.1	70.9	56.3	46.1
O	30.9	29.1	40.1	38.7
N	0	0	3.6	15.2
Si	0	0	0	0

**Interpenetrating polymer networks:** Nanoparticles are particularly active due to their high specific surface area and activation energy<sup>107</sup>. Nanoparticles are stabilized in combination with other materials reducing their effective surface area. In addition, the bulk effect of nanoparticles can give physical, thermal, mechanical, electric, magnetic, optical and phase transition properties to composites. Since nanoparticles are smaller than the wavelength of visible light, their composites may be transparent while the same matrix with larger, normal particles may not. Interpenetrating polymer networks (IPNs) allow mutual enhancement of the properties of two (or more) combined polymers and have been used in many fields. Several authors have studied the effect of nanofillers generated *in situ* in silicone elastomers<sup>108-110</sup> and single-phase polyurethane, but few studies have been devoted to IPN nanocomposites. Nanosize silicon dioxide (65-80 nm) was added to polyurethane/epoxy resin (EP) IPNs<sup>7</sup> to improve mechanical properties by Hongwen *et al.*<sup>111</sup>. The properties and structure of the nanocomposites were studied by dynamic mechanical spectra, scanning electron microscopy (SEM), wide-angle X-ray diffraction (WAXD) and small-angle X-ray scattering (SAXS). Fig. 13a and b show scanning electron photo micrographs. From Fig. 13a it is observed that the black

polyurethane phase constitutes the continuous phase and the white EP phase constitutes a dispersed phase of spheres. The interface of the two phases is very clear. From Figure 13b it is observed that with adding nanosize silicon dioxide, which was treated with a coupling agent, the interface of polyurethane and EP is faint. This is because the coupling agent combined with the matrix and with the nanosize silicon dioxide. Comparing polyurethane/EP = 85/15 and polyurethane/EP/SiO<sub>2</sub> = 85/15/7, it can also be seen that the phase morphology of EP dispersed in polyurethane was changed by the 7 % (w/w) nanosize silicon dioxide. In this system, the average gold particle size of silicon dioxide was 75 nm. The average particle size was gained by SEM from stochastic samples. The system compatibility, which was formed by nanosize silicon dioxide and matrix, was excellent. The silicon oxide dispersed in the IPN homogeneously and aggregates did not appear. This is because the exclusion interaction between the particles, which were treated by surface coupling agent, was increased. Another reason is that the boundary layer of nanocomposites was thicker than that of ordinary composites.

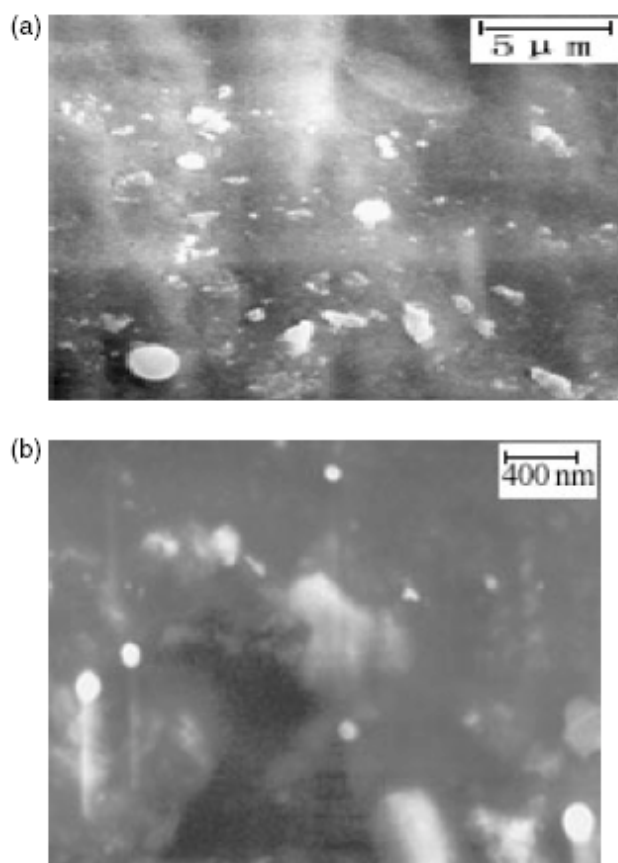


Fig. 13. SEM micrographs of (a) IPN (PU/EP = 85/15), (b) nanocomposite (PU/EP/SiO<sub>2</sub> = 85/15/7) [Ref. 111]

**Silsesquioxane mixture-modified high elongation polyurethane:** Silsesquioxane-based polyurethane (polyurethane/silsesquioxane) hybrid polymers were synthesized by Tao *et al.*<sup>112</sup>. Their idea is that the polyurethane/silsesquioxane is cheap and favourable for mass production, which show significant antithrombogenic qualities as well. They have synthesized a kind of novel mixture silsesquioxane only in one step, which is consisted of three kinds of polyhedral oligomeric silsesquioxane (POSS) compounds. A series of Self-assembled silsesquioxane shows "island" morphology on the polyurethane surface, which successfully reduces platelet adsorption. According to results, the novel silsesquioxane/polyurethane may be a potential blood-contacting biomaterial in the future. Fig. 14 shows FTIR of the silsesquioxane mixture comparing to octvinyl polyhedral oligomeric silsesquioxane (octvinyl POSS). The bands at 1122 and 1043  $\text{cm}^{-1}$  in the mixture silsesquioxane comparing with peak at 1109  $\text{cm}^{-1}$  in the octvinyl POSS represent the stretching vibration two models of Si-O-Si groups cages. The Si-O-Si stretching vibration of  $\text{H}_2\text{C CH-Si-O-Si}$  is 1122  $\text{cm}^{-1}$  and the Si-O-Si stretching vibration of  $\text{HOCH}_2(\text{HO})\text{CHCH}_2\text{OCH}_2\text{CH}_2\text{CH}_2\text{-Si-O-Si}$  is 1043  $\text{cm}^{-1}$  in the mixture silsesquioxane. The double bands in the mixture silsesquioxane cages is similar to the double bands at 1413  $\text{cm}^{-1}$  in the vinyl POSS. Moreover, the strong peaks at 3413  $\text{cm}^{-1}$  show -OH band really exists in the silsesquioxane mixture. The  $^{29}\text{Si}$  NMR spectrum also shows that the  $\text{H}_2\text{C CH-Si}$  groups are at 79 ppm and  $\text{HOCH}_2(\text{HO})\text{CHCH}_2\text{OCH}_2\text{CH}_2\text{CH}_2\text{-Si}$  is at 93.6 ppm in the silsesquioxane mixture comparing with peak at 79 ppm in the octvinyl POSS. These observations further confirm that the silsesquioxane mixture is consists of three kinds of POSS. Fig. 15 is ATR spectrum of polyurethane/silsesquioxane mixture. The stretching

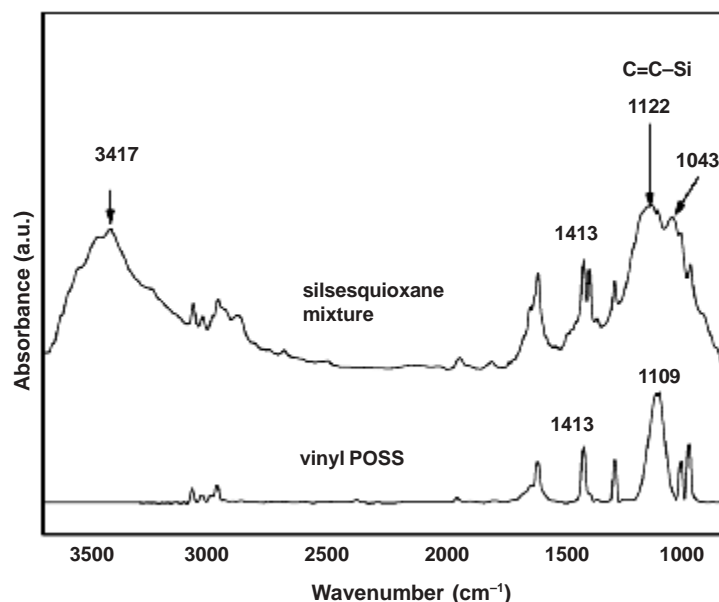


Fig. 14. FTIR of the silsesquioxane mixture comparing to octvinyl poss [Ref. 112]



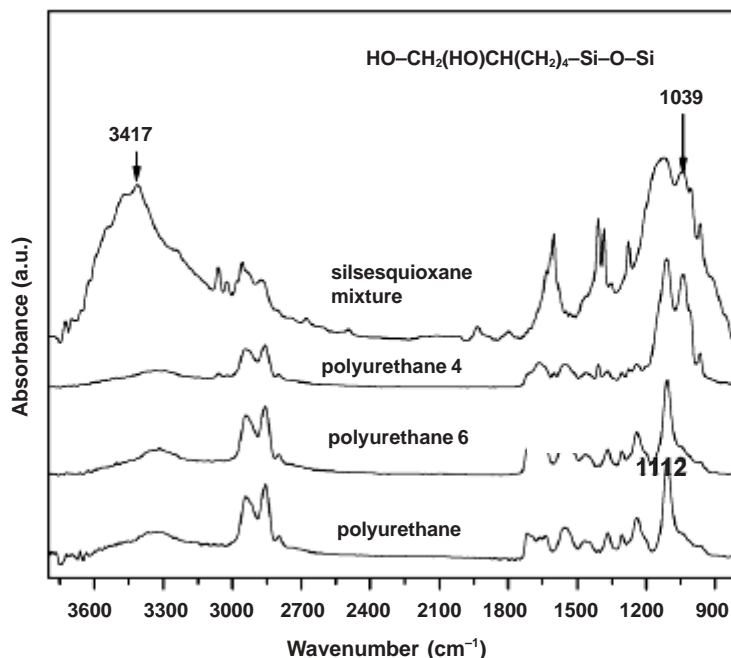


Fig. 15. ATR spectra of the surface polyurethane 6 (wt % = 6 %) and polyurethane 4 (4 %) compare to the silsesquioxane mixture and polyurethane [Ref. 112]

vibrations of the N-H group occurring at 3326 cm<sup>-1</sup> and the carbonyl bands at 1706 cm<sup>-1</sup> are indicative of the presence of urethane moieties. It is worth pointing out that the disappearance of the band at 2275-2250 cm<sup>-1</sup> that is characteristic of isocyanate indicates the completion of the reaction between the hydroxy and the polyurethane prepolymers. The ATR of polyurethane/silsesquioxane (polyurethane 4) mixture has strong HOCH<sub>2</sub>(-HO)CHCH<sub>2</sub>OCH<sub>2</sub>CH<sub>2</sub>CH<sub>2</sub>-Si-O-Si band at 1043 cm<sup>-1</sup> rather than H<sub>2</sub>C CH-Si-O-Si groups at 1122 cm<sup>-1</sup>, which show that pendent-type POSS with Si-O-Si vibration band at 1043 cm<sup>-1</sup> can self-assemble on the surface of the polyurethane/silsesquioxane.

**Effect of nano-silica on the tensile strength of polyurethane:** Figs. 16 and 17 show the effect of nano-silica on the tensile strength and elongation at break of the polyurethane nanocomposites. As the nano-silica content increased up to 3 wt %, both the tensile strength and elongation at break were greatly increased and decreased when the nano-silica content increased further. The enhanced tensile strength of the nanocomposite films can be attributable to the strong interfacial interaction between the polyurethane chains and the nano-silica particles. The elongation at break of the nanocomposite films ( $\approx$  2150 % with 1 wt % nano-silica) was significantly increased as compared to that of pure polyurethane ( $\approx$  630 %). This is an interesting observation, compared to the polyester-based polyurethane-silica nanocomposites where the elongation at break was only slightly enhanced (*e.g.* the maximum elongation at

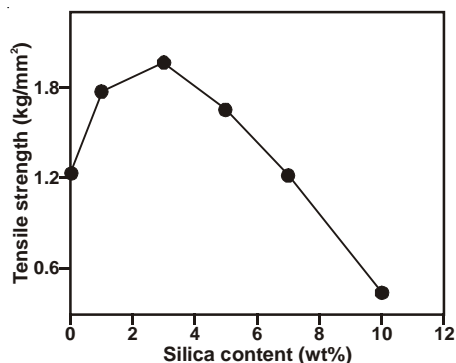


Fig. 16. Tensile strengths of polyurethane-silica nanocomposite films with various silica contents

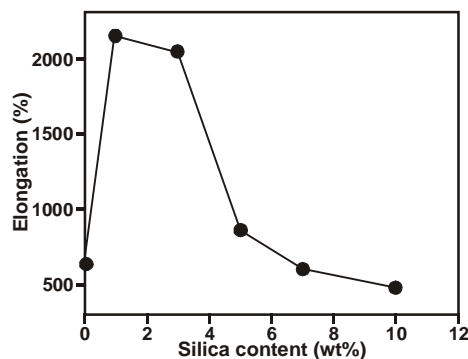


Fig. 17. Elongations at break of polyurethane-silica nanocomposite films with various silica contents

break:  $\approx 220\%$  with 1 wt % nano-silica)<sup>109</sup>. Such a large enhancement in the elongation may be due to the effect of the dispersed nano-silica particles which can act as chain extenders. The decreased tensile strength and elongation at break of the nanocomposites with high contents of the nano-silica (above 5 wt %) may be due to larger aggregates of the nano-silica particles in the polyurethane matrix, as explained for the crystallization behaviour of the poly(tetramethylene glycol) segments.

## Conclusion

In the past decade, material scientists showed great interest in organic-inorganic nanocomposites since their application has dramatically improved material properties in engineering plastics, enhanced rubber, coatings and adhesives. The attractive improvement includes heat resistance, radiation resistance, mechanical and electrical properties, which are usually resulted from the synergistic effect between organic and inorganic components. Effects of different nanoparticles on the properties of polymers vary a lot. Inorganic-organic nanocomposites can be prepared by directly blending organic materials with inorganic nanoparticles or by a sol-gel process with a metal alkoxide such as tetraethoxysilane (TEOS) for the silicon dioxide (SiO<sub>2</sub>)-polymer system. The most commonly used inorganic nanoparticles are SiO<sub>2</sub>, TiO<sub>2</sub>, ZnO and CaCO<sub>3</sub>. It has been well established that the introduction of SiO<sub>2</sub> into a polymer matrix can effectively improve the polymer's properties such as abrasion resistance, shock absorption, surface hardness, modulus and so on. However, it is difficult for nano-silica particles to be dispersed directly in the water phase without a surface pretreatment such as graft modification by a organosilane coupler. Even though they can be dispersed temporarily, the nano-silica particles gather together in larger aggregates finally because of their high surface energy.

Two method was reported in this article to preparation of silicon dioxide/polyurethane. (a) The sol-gel process has been used for the deposition of inorganic minerals *in situ* in an organic polymer matrix. Starting materials for the sol-gel

process are metal alkoxides,  $M(OR)_n$  and a small amount of acid or base as catalyst. Metal alkoxides are hydrolyzed and metal hydroxides,  $M(OH)_n$ , are formed. (b) by Frontal polymerization (FP) which is a mode of converting a monomer into a polymer via a localized reaction zone that propagates through the monomer.

As the silica particles are introduced, the  $T_g$  values of polyurethane/nano-silica composites clearly increase compared with pure polyurethane. The  $T_g$  values of polyurethane/nano-silica composites first increase then decrease as the particle size increases. The maximum  $T_g$  values occur at silica particle sizes within the range of 28-66 nm, which is very consistent with the variation of hydroxyl values at the surfaces of silica particles. It is well established that increasing the nano-silica content can increase the hardness of polyurethane film. The data shows that the hardness first increased and then decreased as the nano-SiO<sub>2</sub> content increased further, no matter how much the film thickness changed. The weight loss gradually decreases as nano-silica content increases, indicating that nano-silica can improve the abrasion resistance of the coating film. As the nano-silica content increased up to 3 wt %, both the tensile strength and elongation at break were greatly increased and decreased when the nano-silica content increased further. The enhanced tensile strength of the nanocomposite films can be attributable to the strong interfacial interaction between the polyurethane chains and the nano-silica particles.

#### ACKNOWLEDGEMENTS

The author is grateful to Iran Khodro Co. and Islamic Azad University for financial supports.

#### REFERENCES

1. C. Hongxiang, Z. Maosheng, S. Hongying and J. Qingming, *Mater. Sci. Eng., A*, **445-446**, 725 (2007).
2. Z. Carsten, T. Ralf, M. Rolf and F. Jurgen, *Adv. Mater.*, **11**, 49 (1999).
3. A.S. Rad and M. Ardjmand, *Chemical Technology: An Indian Journal*, **3** (2008).
4. A.S. Rad and M. Ardjmand, *Chemical Technology: An Indian Journal*, **3** (2008).
5. H. Huang, B. Orler and G.L. Wikes, *Macromolecules*, **20**, 1322 (1987).
6. S. Kohjiya, K. Ochiai and S. Yamashita, *J. Non-Cryst Solids*, **119**, 132 (1990).
7. A. Morikawa, Y. Iyoku, M. Kakimoto and Y. Imai, *Polym. J.*, **24**, 107 (1992).
8. L. Mascia and A. Kioul, *J. Mater. Sci. Lett.*, **13**, 641 (1994).
9. J.H Kim and Y.M. Lee, *J. Membr. Sci.*, **193**, 209 (2001).
10. H.B Park, J.K. Kim, S.Y Nam and Y.M. Lee, *J. Membr. Sci.*, **220**, 59 (2003).
11. P. Jeffrey and M. Krzystof, *Chem. Mater.*, **13**, 3436 (2001).
12. V.W. Timothy and E.P. Timothy, *J. Am. Chem. Soc.*, **123**, 7497 (2001).
13. V.W. Timothy and E.P. Timothy, *J. Am. Chem. Soc.*, **121**, 7409 (1999).
14. S. Spange, *Prog. Polym. Sci.*, **25**, 781 (2000).
15. S. Sankaraiah, L. Jun-Young, C. Sung-Wook and K.J. Hyun, *J. Polym. Sci.: Part B: Polym. Phys.*, **45**, 2747 (2007).
16. J.J. Hwang and H.J. Liu, *Macromolecules*, **35**, 7314 (2002).
17. M. Alexandre and P. Dubois, *Mater. Sci. Eng. R Report*, **28**, 1 (2000).
18. E. Manias, A. Touny, L. Wu, K. Strawhecker, B. Lu and T.C. Chung, *Chem. Mater.*, **13**, 3516 (2001).
19. J. Ren, A.S. Silva and R. Krishnamoorti, *Macromolecules*, **33**, 3739 (2000).
20. J.W. Gilman, C.L. Jackson, A.B. Morgan, R. Jr Harris, E.P. Giannelis and D. Hilton, *Chem. Mater.*, **12**, 1866 (2000).

21. Q. Zhao and E.T. Samulski, *Macromolecules*, **38**, 7967 (2005).
22. H.Y. Byun, M.H. Choi and I.J. Chung, *Chem. Mater.*, **13**, 4221 (2001).
23. Y. Zhu and D.-X. Sun, *J. Appl. Polym. Sci.*, **92**, 2013 (2004).
24. A. Usuki, T. Mizutani, Y. Fukushima, M. Fujimoto and K. Fukumori, U.S. Patent 4,889,885, December 26 (1989).
25. T. Lan, P.D. Kaviratna and T.J. Pinnavaia, *Chem. Mater.*, **7**, 2144 (1995).
26. B. Pourabas and V. Raeesi, *Polymer*, **46**, 5533 (2005).
27. E.P. Giannelis, *Adv. Mater.*, **8**, 29 (1996).
28. P.B. Messersmith and E.P. Giannelis, *J. Polym. Sci. Part A: Polym. Chem.*, **33**, 1047 (1995).
29. L. Biasci, M. Aglietto, G. Ruggeri and F. Ciardelli, *Polymer*, **35**, 3296 (1994).
30. P. Govindaiah, S.R. Mallikarjuna and C. Ramesh, *Macromolecules*, **39**, 7199 (2006).
31. T.C. Chang, Y.T. Wang, Y.S. Hong and Y.S. Chiu, *J. Polym. Sci. Part A: Polym. Chem.*, **38**, 1772 (2000).
32. G. Gorrasi, M. Tortora and V. Vittoria, *J. Polym. Sci. Part B: Polym. Phys.*, **43**, 2454 (2005).
33. D.S. Kim, J.T. Kim and W.B. Woo, *J. Appl. Polym. Sci.*, **96**, 164 (2005).
34. S. SolarSKI, S. Benali, M. Rochery, E. Devaux, M. Alexandre, F. Monteverde and P. Dubois, *J. Appl. Polym. Sci.*, **95**, 238 (2005).
35. H. Goda and C.W. Frank, *Chem. Mater.*, **13**, 2783 (2001).
36. M. Tortora, G. Gorrasi, V. Vittoria, G. Galli, S. Ritrovati and E. Chiellini, *Polymer*, **43**, 6147 (2002).
37. J. Ma, S. Zhang and Z. Qi, *J. Appl. Polym. Sci.*, **82**, 1444 (2001).
38. J. Zhang, R.K. Gupta and C.A. Wilkie, *Polymer*, **47**, 4537 (2006).
39. N.N. Herrera, J.M. Letoffe, J.L. Putaux, L. David and B.L. Elodie, *Langmuir*, **20**, 1564 (2004).
40. Y.Y. Yu and C.Y. Chen, *Polymer*, **44**, 593 (2003).
41. A. Victor and P. Willem, *Polymer*, **43**, 6169 (2002).
42. H. Kaddami, J.F. Gerard, P. Hajji and J.P. Pascault, *J. Appl. Polym. Sci.*, **73**, 2701 (1999).
43. P. Hajji, L. David, J.F. Gerard, J.P. Pascault and G. Vigier, *J. Polym. Sci. B*, **37**, 3172 (1999).
44. T.C. Chang, Y.T. Wang, Y.S. Hong and Y.S. Chiu, *J. Polym. Sci. A*, **38**, 1772 (2000).
45. M.B. Leverkusen, T.E. Koln, S.G. Leverkusen, M. Bock, T. Eng. Bert, S. Groth, B. Klinksek, P. Yeske, G. Jonschker and U. Dellwo, United States Patent 6 020 419 (2000).
46. Z.S. Petrovic and I. Javni, in: Proceedings of the 56th Annu. Tech. Conf.-Soc. Plast. Eng., Vol. 2, pp. 2390-2393 (1998).
47. X.Y. Shang, Z.K. Zhu, J. Yin and X.D. Ma, *Chem. Mater.*, **14**, 71 (2002).
48. Y.T. Wang, T.C. Chang, Y.S. Hong and H.B. Chen, *Thermochim. Acta*, **397**, 219 (2003).
49. T. Ogoshi, H. Itoh, K. Kim and Y. Chujo, *Macromolecules*, **35**, 334 (2002).
50. J.J. Yuan, S.X. Zhou, J.H. Liao and M.W. Li, *Chin. J. Chem. Eng.*, **11**, 483 (2003).
51. Y. Chen and J.O. Iroh, *Chem. Mater.*, **11**, 1218 (1999).
52. Z.C. Pu and J.E. Mark, *Chem. Mater.*, **9**, 2442 (1997).
53. Y.Y. Yu, C.Y. Chen and W.C. Chen, *Polymer*, **44**, 593 (2003).
54. S.X. Zhou, L.M. Wu, J. Sun and W.D. Shen, *Prog. Org. Coat.*, **45**, 33 (2002).
55. Y.Y. Yu, C.Y. Chen and W.C. Chen, *Mater. Chem. Phys.*, **82**, 388 (2003).
56. C.K. Chan, S.L. Peng, I.M. Chu and S.C. Ni, *Polymer*, **42**, 4189 (2001).
57. G.H. Hsiue, W. Kuo, Y.P. Huang and R.J. Jeng, *Polymer*, **41**, 2813 (2000).
58. Y. Gao, N.R. Choudhury and N. Dutta, *Chem. Mater.*, **13**, 3644 (2001).
59. M.N. Xiong, B. You, S.X. Zhou and L.M. Wu, *Polymer*, **45**, 2967 (2004).
60. L. Mascia and A. Kioul, *Polymer*, **36**, 3649 (1995).
61. X.C. Chen, B. You and S.X. Zhou, *Surf. Interface Anal.*, **35**, 369 (2003).
62. L. Chen and J.A. Pojman, *J. Polym. Sci.: Part A: Polym. Chem.*, **43**, 1670 (2005).
63. N.M. Chechilo, R.J. Khvilivitskii and N.S. Enikolopyan, *Dokl Akad Nauk*, **204**, 1180 (1972).
64. N.M. Chechilo and N.S. Enikolopyan, *Dokl Phys. Chem.*, **221**, 392 (1975).
65. N.M. Chechilo and N.S. Enikolopyan, *Dokl Phys. Chem.*, **230**, 840 (1976).
66. J.A. Pojman, J. Willis, D. Fortenberry, V. Ilyashenko and A. Khan, *J. Polym. Sci. Part A: Polym. Chem.*, **33**, 643 (1995).
67. I.P. Nagy, L. Spike and J.A. Pojman, *J. Am. Chem. Soc.*, **117**, 3611 (1995).

68. J.A. Pojman, G. Curtis, V.M. Ilyashenko and A. Khan, *J. Chem. Soc. Faraday Trans.*, **92**, 2825 (1996).
69. J.A. Pojman, W. Elcan, A.M. Khan and L. Mathias, *J. Polym. Sci. Part A: Polym. Chem.*, **35**, 227 (1997).
70. D.I. Fortenberry and J.A. Pojman, *J. Polym. Sci. Part A: Polym. Chem.*, **38**, 1129 (2000).
71. J.A. Pojman, *J. Am. Chem. Soc.*, **113**, 6284 (1991).
72. J.A. Pojman, R. Craven, A. Khan and W. West, *Phys. Chem.*, **96**, 7466 (1992).
73. K.A. Arutiunian, S.P. Davtyan, B.A. Rozenberg and N.S. Enikolopyan, *Dokl Akad Nauk*, **223**, 657 (1975).
74. Y. Chekanov, D. Arrington, G. Brust and J.A. Pojman, *J. Appl. Polym. Sci.*, **66**, 1209 (1997).
75. V.P. Begishev, V.A. Volpert, S.P. Davtyan and A.Y. Malkin, *Dokl Akad Nauk*, **208**, 892 (1973).
76. A. Mariani, S. Fiori, Y. Chekanov and J.A. Pojman, *Macromolecules*, **34**, 6539 (2001).
77. S. Fiori, A. Mariani, L. Ricco and S. Russo, *e-Polymer*, **29**, 1 (2002).
78. A. Mariani, S. Bidali, S. Fiori and M. Sangermano, *J. Polym. Sci. Part A: Polym. Chem.*, **42**, 2066 (2004).
79. J.V. Crivello and B. Falk, *J. Polym. Sci. Part A: Polym. Chem.*, **42**, 1630 (2004).
80. N. Grill, J.A. Pojman, J. Willis and J.B. Whitehead, *J. Polym. Sci. Part A: Polym. Chem.*, **41**, 204 (2004).
81. A. Mariani, S. Bidali, S. Fiori, G. Malucell and E. Sanna, *e-Polymers*, **44**, 1 (2003).
82. S. Bidali, S. Fiori, G. Malucell and A. Mariani, *e-Polymers*, **60**, 1 (2003).
83. M. Jr. Bazile, H.A. Nichols, J.A. Pojman and V. Volpert, *J. Polym. Sci. Part A: Polym. Chem.*, **40**, 3504 (2002).
84. J.A. Pojman, J.R. Willis, A.M. Khan and W. West, *J. Polym. Sci. Part A: Polym. Chem.*, **34**, 991 (1996).
85. J.A. Pojman, A.M. Khan and L. Mathias, *J. Microg. Sci. Technol.*, **10**, 36 (1997).
86. T.K. Chen, Y.I. Tien and K.H. Wei, *Polymer*, **41**, 1345 (2000).
87. G. Kickelbick, *Prog. Polym. Sci.*, **28**, 83 (2003).
88. K.J. Yao, M. Song, D.J. Hourston and D.Z. Luo, *Polymer*, **43**, 1017 (2002).
89. M. Tortora, G. Gorrasi and V. Vittoria, *e-Polymer*, **43**, 6147 (2002).
90. Y.I. Tien and K.H. Wei, *Polymer*, **42**, 3214 (2001).
91. A.M. TorroPalau and G. Fernandez, *J. Adhes Adhes*, **21**, 1 (2001).
92. R.C. Nunes, R.A. Pereira, J.L.C. Fonseca and M.R. Pereira, *Polym. Test*, **20**, 707 (2001).
93. K. Kusakabe and S. Yoneshige, *Morooka*, **149**, 29 (1998).
94. R.C.R. Nunes, J.L.C. Fonseca and M.R. Pereira, *Polym. Test*, **19**, 93 (2000).
95. P.C. LeBaron, Z. Wang and T. Pinnavaia, *J. Appl. Clay Sci.*, **15**, 11 (1999).
96. Y.S. Gu, L. Chen and S. Chen, *Nanjing Gongye Daxue Xuebao*, **25**, 107 (2003).
97. M. Joubert, C. Delaite, E. Bourgeat-Lami and P. Dumas, *J. Polym. Sci. Part A: Polym. Chem.*, **42**, 1796 (2004).
98. L. Wei, T. Tang and B. Huang, *J. Polym. Sci. Part A: Polym. Chem.*, **42**, 941 (2004).
99. C. Chiang, C.M. Ma and H. Kuan, *J. Polym. Sci. Part A: Polym. Chem.*, **41**, 941 (2003).
100. Y. Liu, Y. Wu and W. Ho, *J. Polym. Sci. Part A: Polym. Chem.*, **41**, 2354 (2003).
101. A.A. Kumar, K. Adachi and Y. Chujo, *J. Polym. Sci. Part A: Polym. Chem.*, **42**, 785 (2004).
102. Ch. Xichong and L. Wu, *Polym. Int.*, **52**, 993 (2003).
103. L. Wu, X. Chen, D. Hu and L. Zou, *Surf. Interface Anal.*, **31**, 1094 (2001).
104. Y. Chen, Sh. Zhou, H. Yang and L. Wu, *J. Appl. Polym. Sci.*, **95**, 1032 (2005).
105. S.X. Zhou, L.M. Wu, J. Sun and W.-D. Shen, *J. Appl. Polym. Sci.*, **88**, 189 (2003).
106. S.X. Zhou, L.M. Wu, J. Sun and W.-D. Shen, *Prog. Org. Coat.*, **45**, 33 (2002).
107. SP. Zoran, I. Javni, A. Waddon and G. Banhegyi, *J. Appl. Polym. Sci.*, **76**, 133 (2000).
108. J.E. Mark Ceramic-Reinforced Polymers and Polymer-Modified Ceramics, ANTEC, Toronto, Vol. 2, p. 1810 (1997).
109. D.W. McCarthy, J.E. Mark and D.W. Schaefer, *J. Polym. Sci., Polym. Phys.*, **36**, 1167 (1998).
110. D.W. McCarthy, J.E. Mark and S.J. Klarson, *J. Polym. Sci., Polym. Phys.*, **36**, 1191 (1998).
111. Z. Hongwen, W. Bing and L. Hongtu, *Polym. Int.*, **52**, 1493 (2003).
112. W. Tao, H. Zhou, Y. Zhang and G. Li, *Appl. Surf. Sci.*, **254**, 2831 (2008).